System for integrated interstitial photodynamic therapy and dosimetric monitoring

Johansson, Ann; Thompson, M; Johansson, T; Bendsöe, Niels; Svanberg, Katarina; Svanberg, Sune; Andersson-Engels, Stefan

Published in:
Proceedings of the SPIE - The International Society for Optical Engineering

DOI:
10.1117/12.582892

2005

System for integrated interstitial photodynamic therapy and dosimetric monitoring

Ann Johansson[*a], Marcelo Soto Thompson [a], Thomas Johansson[b], Niels Bendsoe[c], Katarina Svanberg[d], Sune Svanberg [a], Stefan Andersson-Engels [a]

[a]Department of Atomic Physics, Lund Institue of Technology, PO Box 118, SE-221 00 Lund, Sweden
[b]SpectraCure AB, Ideon Research Park, Ole Römers väg 16, SE-223 70 Lund, Sweden
[c]Department of Dermatology, Lund University Hospital, SE-221 85 Lund, Sweden
[d]Department of Oncology, Lund University Hospital, SE-221 85 Lund, Sweden

ABSTRACT

Photodynamic therapy for the treatment of cancer relies on the presence of light, sensitizer and oxygen. By monitoring these three parameters during the treatment a better understanding and treatment control could possibly be achieved. Here we present data from *in vivo* treatments of solid skin tumors using an instrument for interstitial photodynamic therapy with integrated dosimetric monitoring. By using intra-tumoral ALA-administration and interstitial light delivery solid tumors are targeted. The same fibers are used for measuring the fluence rate at the treatment wavelength, the sensitizer fluorescence and the local blood oxygen saturation during the treatment. The data presented is based on 10 treatments in 8 patients with thick basal cell carcinomas. The fluence rate measurements at 635 nm indicate a major treatment induced absorption increase, leading to a limited light penetration at the treatment wavelength. This leads to a far from optimal treatment since the absorption increase prevents peripheral tumor regions from being fully treated. An interactive treatment has been implemented assisting the physician in delivering the correct light dose. The absorption increase can be compensated for by either prolonging the treatment time or increasing the output power of each individual treatment fiber. The other parameters of importance, i.e. the sensitizer fluorescence at 705 nm and the local blood oxygen saturation, are monitored in order to get an estimate of the amount of photobleaching and oxygen consumption. Based on the oxygen saturation signal, a fractionized irradiation can be introduced in order to allow for a re-oxygenation of the tissue.

Keywords: photodynamic therapy, interstitial, ALA, PpIX, dosimetry, photobleaching, tissue oxygen saturation, tissue absorption, diagnostic, system

1. INTRODUCTION

In the search for new treatment modalities for cancer treatment, photodynamic therapy (PDT) has shown promising results in terms of selectivity and efficacy[1, 2]. PDT relies on the presence of a photosensitizing agent, for example δ-aminolevulinic acid (ALA)-derived protoporphyrin IX (PpIX), which once activated by light of the appropriate wavelength generates cytotoxic species, mostly singlet oxygen and oxygen radicals. Tissue necrosis is caused by a combination of immediate cell death and apoptosis induced by these radicals and indirect damage to the vascular system[3, 4]. ALA-mediated PDT has been successfully used in the treatment of superficial lesions in the skin, bladder and aerodigestive tract and for the treatment of actinic keratosis[5].
Interstitial light delivery via optical fibers has been pursued by many groups[6, 7], opening up the possibility to treat also thicker and deeper lying tumors. An additional advantage of interstitial delivery of the therapeutic irradiation using multiple fibers is that it facilitates treatment of irregularly shaped lesions, while sparing normal surrounding tissue.

[*] Ann.Johansson@fysik.lth.se; phone +46 46 2223120; fax +46 46 2224250; http://www-atom.fysik.lth.se/

Optical Methods for Tumor Treatment and Detection: Mechanisms and Techniques in Photodynamic Therapy XIV, edited by David Kessel, Proceedings of SPIE Vol. 5689 (SPIE, Bellingham, WA, 2005) · 1605-7422/05/$15 · doi: 10.1117/12.582892

The light distribution during interstitial PDT depends on the tissue optical properties and tissue inhomogeneities can greatly influence the deposited light dose in different tumor regions. Another factor one has to take into account is any treatment induced changes of the tissue structure and tissue optical properties, such as edema, changes in blood flow and tissue oxygenation or hyperthermia.
The tissue response to PDT is tightly connected to the oxygenation of the tissue, where a good oxygen access leads to a better treatment outcome. For ALA-mediated PDT, a high irradiance at the therapeutic wavelength has been shown to induce less extensive tissue damage, an effect that has been explained by oxygen depletion occurring at the higher irradiances[8, 9]. Besides inhibiting the photodynamic reaction, oxygen depletion also affects the light transmission in tissue. During a PDT treatment session the tumor is gradually de-oxygenated, which based on the higher absorption coefficient of deoxy-hemoglobin as compared to oxy-hemoglobin, would lead to a decrease in light transmission throughout the tumor volume. Studies by Foster *et al.* have shown up to 15-fold increase in light penetration at 630 nm when comparing a hypoxic to a well-oxygenated tissue phantom containing human erythrocytes[10]. These results further emphasize the need for a good tumor oxygenation level as de-oxygenated tissue limits light penetration and prevents the entire tumor volume from receiving a sufficient light dose.
The treatment induced sensitizer photobleaching is an oxygen dependent process, where the initial rate of sensitizer photobleaching correlates well with the tissue oxygenation. Therefore it has been suggested that studying the rate of sensitizer photobleaching could be a useful dosimetric tool in trying to predict the treatment outcome[11].

An accurate dosimetry model, which takes the fluence rate distribution within the tissue volume of interest, the sensitizer concentration and the tissue oxygenation into account, is of major importance in interstitial photodynamic therapy. Recently we have reported on the construction and initial clinical testing of an instrument for interstitial photodynamic therapy which allows for diagnostic measurements in order to monitor the treatment progression[12]. The six optical fibers used for delivery of the therapeutic irradiation are also utilized in order to monitor the fluence rate at the treatment wavelength, the protoporphyrin IX fluorescence and the tissue oxygen saturation during the treatment session. Here we present data from monitoring tissue light transmission changes during 10 treatment sessions and what this might have for consequences on treatment outcome. Also, results from measuring the protoporphyrin IX photobleaching and the oxy- and deoxy-hemoglobin concentration changes are presented.

2. MATERIAL AND METHODS

2.1. Instrumentation

An instrument for interstitial photodynamic therapy has been used, where a maximum of six bare end optical fibers are utilized to deliver the therapeutic light into the tumor mass, see Figure 1[12]. The same fibers can also be used in order to perform diagnostic measurements during the treatment session.

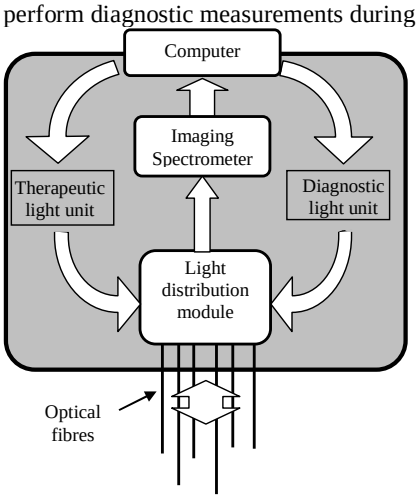

Figure 1. Schematic describing the overall instrument layout.

While in treatment mode, light from the therapeutic light unit, which consists of six diode lasers, each emitting a maximum of 200 mW at 635 nm, is guided into the light distribution module and coupled into the six 400 μm diameter

patient fibers. During a treatment session, the therapeutic irradiation is repeatedly interrupted in order to perform measurements of diagnostic importance. In measurement mode, light from the diagnostic light unit is coupled into one of the patient fibers via the light distribution module. After interacting with the tissue some of the light is detected by the remaining five fibers and coupled into an imaging spectrometer covering the spectral range 620-810 nm. One measurement sequence involves successively coupling the output from the two diagnostic light sources into each and every one of the six patient fibers.

The first diagnostic light source is a diode laser similar to the treatment lasers. Upon emission from one of the patient fibers the light transmission at 635 nm to the other five fibers is monitored as a function of the delivered light dose. This measurement monitors changes in light transmission, which might be a consequence of e.g. bleeding at the fibre tips, variations in tissue oxygen saturation, changes in blood flow or blood volume, and an insufficient treatment may thus be prevented by re-inserting fibers or compensating for possible transmission variations by adjusting the treatment time. The 635 nm irradiance also induces PpIX fluorescence at 705 nm throughout the tumour volume. This signal is monitored simultaneously to the light transmission at the therapeutic wavelength and is used to study the rate of PpIX photobleaching.

The other diagnostic light source is a light emitting diode covering the spectral range between 760 and 810 nm. The transmission in between patient fibers is used to assess the optical density within this wavelength interval,

$$\mathrm{A(t)} = -\log\frac{S(\mathrm{t})}{S_0}, \tag{1}$$

where S_0 is the initial light transmission and *S(t)* is the light transmission as detected during the subsequent measurement sequences. The measurement of *A(t)* is used to monitor changes in oxy- and deoxy-hemoglobin concentration by means of the modified Beer-Lambert law and least squares fitting. According to the modified Beer-Lambert law, which is an empirical description of light attenuation in scattering media, the change in optical density can be expressed as

$$\Delta A = \sum_i \left(\varepsilon_i \Delta c_i(t)\right) \cdot DPF \cdot L, \tag{2}$$

where ε [M^{-1} cm^{-1}], c [M] and L [cm] are the extinction coefficient of the medium, the concentration of the absorbing component and the source detector separation, respectively. The summation is taken over all absorbing chromophores, *i*.In the following analysis we assume oxy- and de-oxy hemoglobin are the only chromophores whose absorption might change during the treatment and that any light transmission changes are due to changes in the concentration of these two tissue constituents. *DPF* is the differential pathlength factor, which is dependent on wavelength, tissue type and measurement geometry. By assuming that *DPF* remains constant during the treatment session one can use equation (3) below to relate the measured optical density changes to relative chromophore concentration changes[13, 14],

$$\Delta A = -\log\frac{S_{final}}{S_0} = \left(\varepsilon_{Hb}\Delta[Hb] + \varepsilon_{HbO}\Delta[HbO]\right) \cdot DPF \cdot L, \tag{3}$$

where ε_{HbO} and ε_{Hb} are the wavelength dependent extinction coefficients of oxy- and deoxy-hemoglobin, respectively. By measuring the tissue optical density changes and using the known extinction coefficients of oxy- and deoxy-hemoglobin within a certain wavelength interval[15], the changes of these chromophores can be calculated.
In order to derive equation (3) several assumptions have been made. First, one has to assume a scattering coefficient that remains constant over time and that is much larger in magnitude than the absorption coefficient. Second, Equation (3) is valid only for small and global concentration changes in homogenous tissues. Finally, *DPF* requires knowledge of the initial absorption and scattering coefficients, which in this work have been chosen according to Table 1.

The above analysis is not only used to assess the oxy- and deoxy-hemoglobin concentration changes. Based on the known extinction coefficients of oxy- and deoxy-hemoglobin, the changes in light transmission at the treatment wavelength can be approximated by extrapolating the measured optical density changes from the wavelength region 760-810 nm down to 635 nm. The motivation for doing this extrapolation is to check whether the treatment induced absorption changes as reported on in this paper are due to changes in tissue oxygenation, blood flow and blood volume.
By monitoring the treatment induced changes in tissue oxygen saturation a fractionized irradiation might be introduced in order to allow for an increased oxygen inflow to the treated region.

2.2. Patients

The study included 8 patients with thick skin lesions and was approved by the Local Ethics Committee at the Lund University Hospital. Five lesions were diagnosed as nodular basal cell carcinomas, whereas the remaining three lesions were diagnosed as superficial basal cell carcinoma, squamous cell carcinoma and keratoacanthoma/squamous cell carcinoma. Two of the patients diagnosed with basal cell carcinomas underwent two treatment sessions, resulting in a total of 10 treatment sessions performed.

At the time of treatment the tumor geometry was determined visually and by palpation by an experienced oncologist. The lesion was photosensitized by mixing ALA (5-aminolevulinic acid, MEDAC GmbH, Hamburg, Germany) into an oil-in water emulsion (Essex Cream, Schering Corp., Kenilworth, USA) to a concentration by weight of 20 %, which was applied topically with a 10-mm margin to the lesion 4-6 hours before the therapeutic irradiation. An occlusive dressing (Tegaderm™, 3M, UK) was used in order to prevent the cream from smearing and an ordinary dressing shielded the area from ambient light prior to the treatment irradiation. Thirty minutes prior to the treatment, three patients were also given ALA intra-tumorally by dissolving 1.5 g ALA powder in 10 ml 0.9% saline buffer. Prior to the therapeutic irradiation the lesion was prepared according to clinical praxis by disinfecting the treatment area, and subsequently administering Xylocain (AstraZeneca, Södertälje, Sweden) subcutaneously as anesthetics. The six sterilized patient fibers were inserted and subsequently fixed in a holder which in turn was attached to the patient stretcher. The fiber positions were chosen to get as homogenous a light distribution inside the lesion as possible while sparing the surrounding tissue.

In order to get an approximate prediction of the treatment times necessary, the fluence rate, $\phi(\mathbf{r})$, within the lesion was determined by solving the steady-state diffusion equation[16],

$$\nabla^2\phi(\mathbf{r}) - \mu_{eff}^2\phi(\mathbf{r}) = \sum_i S(\mathbf{r}_i), \qquad (4)$$

where $\mu_{eff} = [\,3\mu_a(\mu_a + \mu_s')\,]^{1/2}$, μ_a and μ_s' are the effective attenuation, absorption and reduced scattering coefficients. For this prediction, the values in Table 1 were chosen for these parameters[17]. The source term, $\sum S(\mathbf{r}_i)$ was modelled as isotropic point sources, denoted by the index *i*. A commercial program (FEMLab®, Comsol, Sweden) was used to model the fluence rate distribution by using the finite element method. For the case of superficial lesions, the extrapolated boundary condition was used. Based on the fluence rate distribution, the absorbed dose throughout the tumour volume was calculated. With a threshold (15 Jcm^{-3})[18] for the absorbed light dose considered sufficient for inducing cell necrosis, an estimate of the necessary treatment time was calculated.

Tissue type	μ_a (cm^{-1})	μ_s' (cm^{-1})
normal	0.16	12.0
tumor	0.31	12.4

Table 1. Tissue optical properties used in modeling the light distribution.

Individual fiber output powers were kept constant throughout the treatment session at power levels ranging from 25 to 100 mW. The therapeutic irradiation was interrupted with varying time intervals (30-120 s) in order to perform the measurement sequences (approx. 45 s). Measurement sequences were performed more frequently at the beginning of the treatment session in order to follow the rapid sensitizer photobleaching and also prior to and at the end of the treatment session.

3. RESULTS

Using the first diagnostic light source, the spectra recorded via the other five fibers typically looked like the inset in Figure 2. A signal describing the light transmission as a function of delivered light dose was obtained by summing the detected signal within the spectral interval 625 to 645 nm for each measured spectrum. Figure 2 shows three examples of the light transmission temporal profiles where the signals have been normalized to their respective initial values. Curves I and II display varying absorption changes during the treatment session, whereas curve III could possibly be explained by blood pooling at the fiber tip. Data with characteristics of curve III, i.e. a rapid loss of signal resulting in an insufficient signal-to-noise ratio were excluded from further data analysis. Out of a total of 60 fiber insertions in 10 patients, possible blood pooling at the fiber tips could be identified in 4 cases.

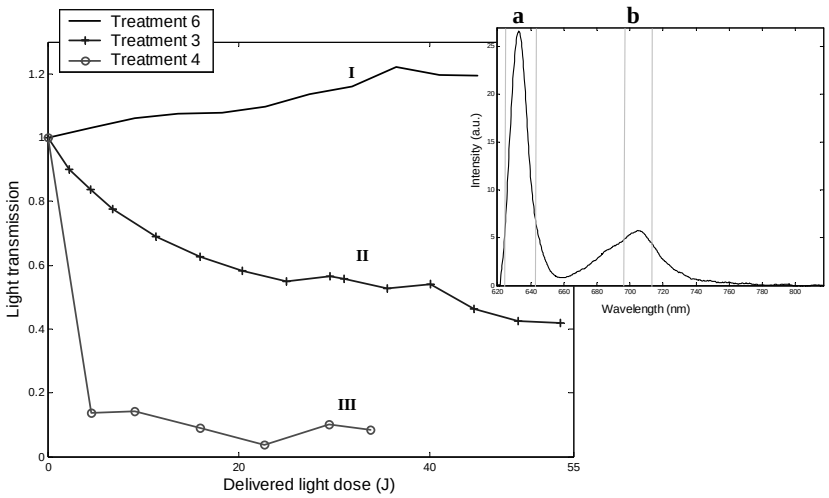

Figure 2. Three illustrations of light transmission variations between patient fibers from three different treatment sessions. Inset shows raw data, where dashed vertical lines indicate spectral region for studying light transmission signal (a) and sensitizer fluorescence (b).

All treatment sessions were performed using six patient fibers positioned approximately equidistantly around the tumor center. Measuring the light transmission between all possible fiber combinations results in 30 signals from each measurement sequence. If only looking at transmission signals between neighbouring fibers, i.e. 12 signals, it is easier to identify lesion inhomogeneities and follow changes in optical properties with only minor influence of source-detector separations. Figure 3 shows the average of the light transmission between neighbouring fibers during one treatment session after normalizing each signal to its initial value. Judging by the size of the error bars, which denote standard deviations, the decrease in light transmission was rather homogenous within the entire tumor volume. An immediate result of the absorption increase and the thereby limited light distribution is that the entire tumor volume did not receive a light dose above the predefined threshold supposed to be required in order to produce tissue necrosis. Assuming that it is only a change in the absorption coefficient that cause the decreasing signal in Figure 3 and that the change is homogenous within the entire tumor volume, one can calculate the change in absorption coefficient as a function of the treatment time. Using this information, it is possible to model the actual light distribution and thereby re-calculate the expected treatment volume. This analysis relies on the validity of the diffusion equation and use of the extrapolated boundary condition for the case of superficial lesions. For the case illustrated in Figure 3, the absorption coefficient was found to increase by 73 ±15 %, which resulted in a treated volume at the end of the treatment session as illustrated in Figure 4. The figure shows a cross section through the middle part of the tumor and clearly, the entire volume was not fully treated.

A significant treatment induced absorption increase was established in 8 of 9 treatments by performing a one-sided Student's *t*-test, where $P<0.02$ was considered significant. Figure 5 shows the mean of the remaining light transmission at the end of the treatment sessions. The data displayed was achieved by averaging the light transmission between neighbouring patient fibers from the last measurement sequence in each treatment session. The varying light transmission change could not be explained only by the different inter-fiber distances used in the individual treatments. Data from treatment session 4 has been excluded since the optical fibers lost their original positions when the patient started coughing after 240 s of therapeutic irradiation.
In a similar manner as when calculating the actual absorbed light dose for Figure 4, the actual light dose in the tumor bed has been calculated and compared to the planned light dose as modeled before the treatment session. The result of this comparison is shown in Table 2, where the minimum of the actual light dose in the tumor bed is expressed as a percentage of the minimum of the planned light dose.

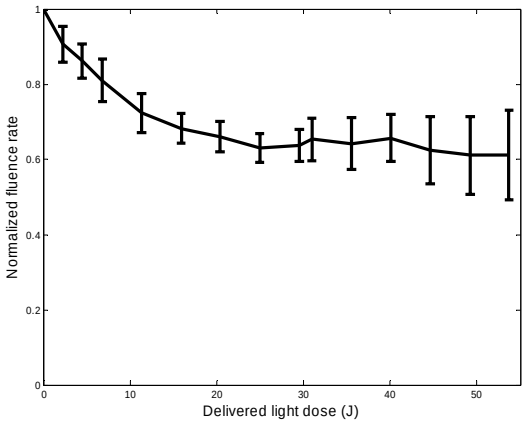

Figure 3. Average of normalised light transmission between patient fibers from one patient.

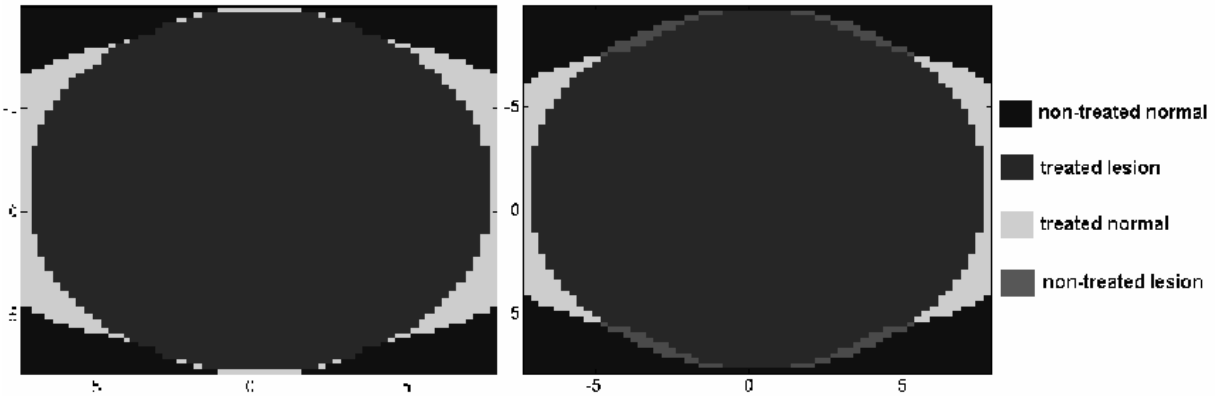

Figure 4. Tumor cross sections at the end of the treatment session. Figure to the left shows treated regions when assuming a constant absorption coefficient throughout the treatment session, whereas in the rightmost figure the calculations for the absorbed dose are based on transmission changes as displayed in Figure 3.

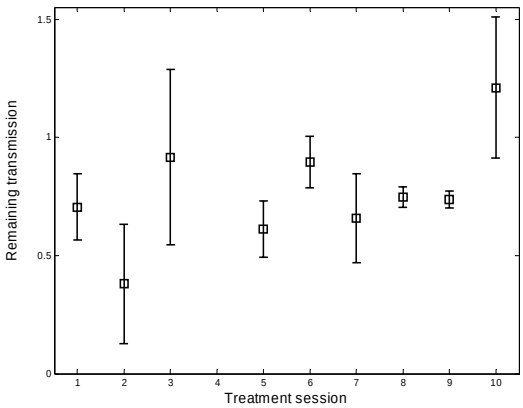

Figure 5. Average of remaining light transmission for 9 treatment sessions. Data is based on light transmission signals between neighbouring fibers and error bars denote standard deviations.

Treatment session	Delivered light dose (% of planned light dose)
1	75
2	44
3	90
4	-
5	70
6	84
7	65
8	80
9	74
10	97

Table 2. Actual delivered light dose as percentage of planned light dose.

In order to quantify the PpIX photobleaching, the signal within the spectral interval *b* (695-715 nm) as indicated by the inset in Figure 2 is studied after subtracting a constant background off-set. A typical sensitizer photobleaching curve is shown in Figure 6, where the average of the normalized fluorescence signal as detected via the patient fibers in one patient has been plotted as a function of the delivered light dose. Again, the error bars denote one standard deviation above and one below the average signal. Data from the treatment sessions display a rapid initial photobleaching followed by a slowly decaying fluorescence level. One should observe that the evaluated sensitizer fluorescence signal has not been compensated for the absorption increase as seen from the fluence rate measurements.

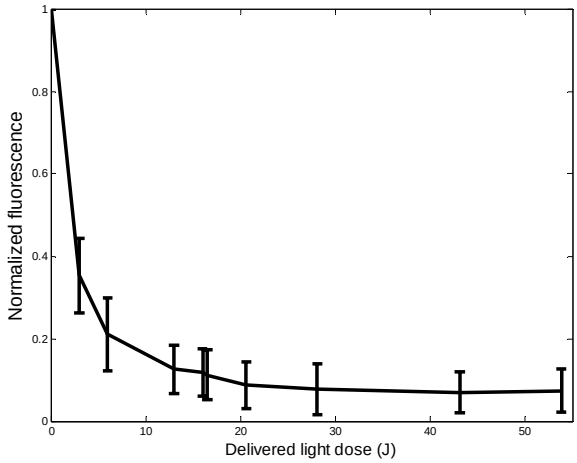

Figure 6. PpIX fluorescence as a function of delivered light dose. Data represents the average signal from one of the treatment sessions.

With the second diagnostic light source emitting, the recorded raw spectra were evaluated according to Equation (3) in order to assess variations in oxy- and deoxy-hemoglobin concentration. Figure 7.a shows the evaluated tissue optical density for a few selected treatment times. Figure 7.b illustrates the corresponding concentration changes of oxy- and deoxy-hemoglobin. Using the known extinction coefficients of oxy- and deoxy-hemoglobin, these signals were also used in order to predict the variation in light transmission at 635 nm between the patient fibers. Figure 7.c illustrates the agreement between the measured light transmission at 635 nm and the transmission curves predicted by extrapolating the calculated absorbance at 760-810 nm for one pair of patient fibers during one treatment session.

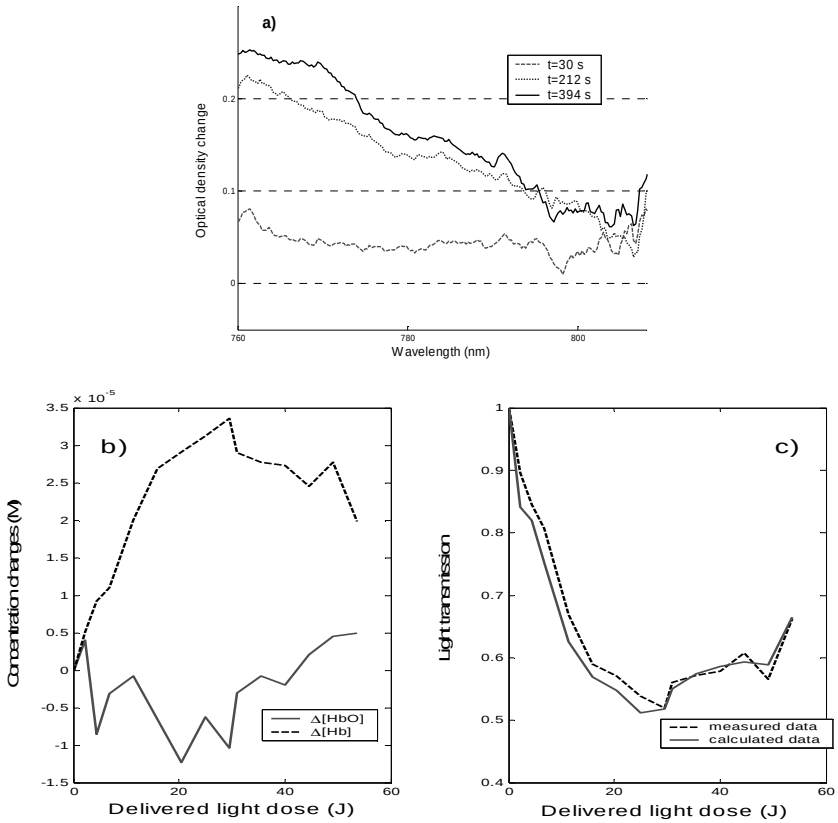

Figure 7.a) Measured optical density in the wavelength interval 760 to 810 nm. b) Oxy- and deoxy-hemoglobin changes as a function of the delivered light dose. c) Measured (solid) and calculated (dashed) light transmission. Calculations are based on data according to a) and b).

4. DISCUSSION

Using a recently developed system for interstitial photodynamic therapy, we have monitored light transmission changes, sensitizer photobleaching and hemoglobin concentration changes within the treated tissue during treatment of thick skin lesions.

When addressing the therapeutic light transmission within the tumor, the most important aspect is whether there is blood pooling at the fiber tips. Because of the high absorption coefficient of blood, local bleeding was easily recognized by a marked loss of light transmission. Judging by the huge impact blood absorption has on the light distribution within the tissue, it is of great importance to monitor this parameter.

After excluding data influenced by local bleeding or characterized by an insufficient signal-to-noise ratio, a significant treatment induced absorption increase was found in 9 of 10 treatment sessions. The absorption increase influences the volume that is treated, as illustrated in Figure 4 for one of the treatment sessions. Figure 5 shows that the degree of absorption increase varies among patients, which further indicates that there is need for individual monitoring of the light distribution within the lesion during treatment.

Other groups have also reported on a decrease in light transmission in tissue during PDT[19-21] and possible explanations include damage to the tissue microcirculation[21], alteration of the local blood flow and perfusion[19], local hyperthermia or tissue de-oxygenation as a result of the oxygen consumption[10, 19]. Here we have tested the hypothesis that changes in tissue oxygen saturation and blood volume result in the observed tissue absorption increase. Since deoxy-hemoglobin is a much stronger absorber at 635 nm than oxy-hemoglobin, de-oxygenation will results in an increase of the tissue absorption. By measuring the optical density in the wavelength range 760 to 810 nm and using the modified Beer-

Lambert law, variations in oxy- and deoxy-hemoglobin concentration have been calculated. By extrapolating the absorbance in this NIR wavelength range to 635 nm it is possible to compare the changes in light transmission predicted by the calculated changes in hemoglobin concentration to those actually measured at 635 nm. For some patients this comparison shows excellent agreement, emphasizing the importance of well oxygenated tissue not only for production of toxic radicals but also for enabling a sufficient light distribution throughout the tumor volume.
In many cases, the data analysis also indicates a change in blood volume. PDT is often associated with vascular shutdown[22, 23] and vasoconstriction has also been noticed using ALA-induced PpIX as photosensitizer, especially with systemic drug administration[24]. In the case of topical or intra-tumoral ALA application, these effects on the blood perfusion are not as pronounced[25, 26]. In this study it is more likely that the blood volume increased as a consequence of tissue inflammatory response and/or damage to tissue microcirculation. In the latter case, blood stasis could result from microagglutination of red blood cells[27], thereby increasing the average concentration of red blood cells.

As shown in Figure 6, the PpIX fluorescence displays a rapid initial photobleaching followed by a more slowly decaying fluorescence level. Although not shown here, the signal is well described by a sum of two exponential terms, where the exponent of the rapidly vanishing term can be used to quantify the initial rate of photobleaching. König *et al.*[28] have suggested using the rate of sensitizer photobleaching as a dosimetric tool in trying to predict the treatment outcome.
Although using another sensitizer than ALA-induced PpIX, Woodhams *et al.*[22] have observed a drop in oxygen saturation in regions where tissue necrosis was found post treatment. The authors have speculated whether is it possible to use real-time monitoring of oxygen saturation during PDT in order to improve the treatment outcome.
The importance of a well oxygenated tissue during PDT has also been shown by Curnow *et al.*[9], who reported up to three times more necrosis when using fractionated as compared to continuous irradiation. The effect has been explained by improved oxygen inflow to the treatment volume. Based on the results presented here and on the work presented by these references, it seems highly desirable to implement real-time dosimetry during PDT.

In summary, we have reported on real-time measurement of light transmission during interstitial PDT *in vivo*. The data indicate treatment induced changes of the tissue optical properties, where the effect this has on the light distribution is of great importance for the treatment outcome. Also, by monitoring the sensitizer photobleaching and the tissue oxygen saturation, it might be possible to introduce treatment feed-back with the ultimate goal of treatment outcome improvement.

ACKNOWLEDGEMENTS

The project was financially supported by the Swedish Foundation for Strategic Research and also by Karolinska Development AB, Stockholm and Lund University Developmental AB through SpectraCure AB, Lund. The authors wish to thank Dr Sara Pålsson for contributing to the scientific discussions and Epsilon Technology AB for their aid in assembling the hardware.

REFERENCES

1. S. L. Marcus, "Photodynamic therapy of human cancer: clinical status, potential and needs,"*Future Directions and Applications in Photodynamic Therapy,* C. J. Gomer, ed.,pp 5-56, Soc. Photo-Opt. Instrum. Eng., (1990).
2. J. C. Kennedy, R. H. Pottier, and D. C. Pross, "Photodynamic therapy with endogenous protoporphyrin IX: Basic principles and present clinical experience," *J. Photochem. Photobiol. B.* **6**, 143-148 (1990)
3. B. B. Noodt, K. Berg, T. Stokke, Q. Peng, and J. M. Nesland, "Apoptosis and necrosis induced with light and 5-aminolaevulinic acid-derived protoporphyrin IX," *Br. J. Cancer* **74**(1), 22-29 (1996)
4. D. J. H. Roberts, F. Cairnduff, I. Driver, B. Dixon, and S. B. Brown, "Tumor vascular shutdown following photodynamic therapy based on polyhematoporphyrinor 5-aminolevulinic acid," *Int. J. Oncol.* **5**(4), 763-768 (1994)
5. Q. Peng, T. Warloe, K. Berg, J. Moan, M. Kongshaug, K.-E. Giercksky, and J. M. Nesland, "5-aminolevulinic acid-based photodynamic therapy: Clinical research and future challenges," *Cancer* **79**, 2282-2308 (1997)
6. P. J. Lou, H. R. Jager, L. Jones, T. Theodossy, S. G. Bown, and C. Hopper, "Interstitial photodynamic therapy as salvage treatment for recurrent head and neck cancer," *Br. J. Cancer* **91**(3), 441-446 (2004)

7. S. F. Purkiss, M. F. Grahn, A. M. Abulafi, R. Dean, J. T. Allardice, and N. S. Williams, "Multiple Fiber Interstitial Photodynamic Therapy of Patients with Colorectal Liver Metastases," *Lasers Med. Sci.* **9**(1), 27-35 (1994)
8. D. J. Robinson, H. S. de Bruijn, N. van der Veen, M. R. Stringer, S. B. Brown, and W. M. Star, "Fluorescence photobleaching of ALA-induced protoporphyrin IX during photodynamic therapy of normal hairless mouse skin: The effect of light dose and irradiance and the resulting biological effect," *Photochem. Photobiol.* **67**(1), 140-149 (1998)
9. A. Curnow, J. C. Haller, and S. G. Bown, "Oxygen monitoring during 5-aminolaevulinic acid induced photodynamic therapy in normal rat colon. Comparison of continuos and fractionated light regimes.," *J. Photochem. Photobiol. B.* **58**(2-3), 149-155 (2000)
10. M. Soumya and T. H. Foster, "Carbogen breathing significantly enhances the penetration of red light in murine tumours *in vivo*," *Phys. Med. Biol.* **49**(10), 1891-1904 (2004)
11. J. C. Finlay, D. L. Conover, E. L. Hull, and T. H. Foster, "Porphyrin bleaching and PDT-induced spectral changes are irradiance dependent in ALA-senstitized normal rat skin in vivo," *Photochem. Photobiol.* **73**(1), 54-63 (2001)
12. Soto Thompson, M., Johansson, A., Johansson, T., Andersson-Engels, S., Bendsoe, N., Svanberg, K., and Svanberg, S. "Clinical system for interstitial photodynamic therapy with combined on-line dosimetry measurements", 2004, Unpublished Work
13. D. A. Boas, T. Gaudette, G. Strangman, X. F. Cheng, J. J. A. Marota, and J. B. Mandeville, "The accuracy of near infrared spectroscopy and imaging during focal changes in cerebral hemodynamics," *Neuroimage* **13**(1), 76-90 (2001)
14. A. D. Edwards, G. C. Brown, M. Cope, J. S. Wyatt, D. C. McCormick, S. C. Roth, D. T. Delpy, and E. O. R. Reynolds, "Quantification of concentration changes in neonatal human cerebral oxidized cytochrome oxidase," *J. Appl. Physiol.* **71**(7), 1907-1913 (1991)
15. Prahl, S. A. Optical Absorption of Hemoglobin. Oregon Medical Laser Center . 2004.
Ref Type: Electronic Citation
16. K. M. Case and P. F. Zweifel, *Linear transport theory*, Addison-Wesley Publishing Co., Reading, MA (1967)
17. J. B. Fishkin, O. Coquoz, E. R. Anderson, M. Brenner, and B. J. Tromberg, "Frequency-domain photon migration measurements of normal and malignant tissue optical properties in a human subject," *Appl. Opt.* **36**(1), 10-20 (1997)
18. T. Johansson, M. Soto Thompson, M. Stenberg, C. af Klinteberg, S. Andersson-Engels, S. Svanberg, and K. Svanberg, "Feasibility study of a novel system for combined light dosimetry and interstitial photodynamic treatment of massive tumors," *Appl. Opt.* **41**(7), 1462-1468 (2002)
19. Q. Chen, B. C. Wilson, S. D. Shetty, M. S. Patterson, J. C. Cerny, and F. W. Hetzel, "Changes in in vivo optical properties and light distributions in normal canine prostate during photodynamic therapy," *Radiat. Res.* **147**(1), 86-91 (1997)
20. J. P. A. Marijnissen and W. M. Star, "Quantitative light dosimetry in vitro and in vivo," *Lasers Med. Sci.* **2**, 235-242 (1987)
21. A. M. K. Nilsson, R. Berg, and S. Andersson-Engels, "Measurements of the optical properties of tissue in conjunction with photodynamic therapy," *Appl. Opt.* **34**(21), 4609-4619 (1995)
22. J. H. Woodhams, L. Kunz, S. G. Bown, and A. J. MacRobert, "Correlation of real-time haemoglobin oxygen saturation monitoring during photodynamic therapy with microvascular effects and tissue necrosis in normal rat liver," *Br. J. Cancer* **91**(4), 788-794 (2004)
23. I. P. J. van Geel, H. Oppelaar, P. F. J. W. Rijken, H. J. J. A. Bernsen, N. E. M. Hagemeier, A. J. van der Kogel, R. J. Hodgkiss, and F. A. Stewart, "Vascular perfusion and hypoxic areas in RIF-1 tumours after photodynamic therapy," *Br. J. Cancer* **73**, 288-293 (1996)
24. K. Svanberg, D. L. Liu, I. Wang, S. Andersson-Engels, U. Stenram, and S. Svanberg, "Photodynamic therapy using intravenous δ-aminolaevulinic acid-induced protoporphyrin IX sensitisation in experimental hepatic tumours in rats," *Br. J. Cancer* **74**, 1526-1533 (1996)
25. I. Wang, S. Andersson-Engels, G. E. Nilsson, K. Wårdell, and K. Svanberg, "Superficial blood flow following photodynamic therapy of malignant skin tumours measured by laser Doppler perfusion imaging," *Br. J. Dermatol.* **136**, 184-189 (1997)
26. S. Pålsson, L. Gustafsson, N. Bendsoe, M. Soto Thompson, S. Andersson-Engels, and K. Svanberg, "Kinetics of the superficial perfusion and temperature in connection with photodynamic therapy of basal cell

carcinomas using esterified and non-esterified 5-aminolevulinic acid," *Br. J. Dermatol.* **148**(6), 1179-1188 (2003)
27. A. Castellani, G. P. Pace, and M. Concioli, "Photodynamic effect of haematoporphyrin on blood circulation," *J. Path. Bact.* **86**, 99-102 (1963)
28. K. König, H. Schneckenburger, A. Rück, and R. Steiner, "*In vivo* photoproduct formation during PDT with ALA-induced endogenous porphyrins," *J. Photochem. Photobiol. B.* **18**, 287-290 (1993)